Materials and Design 182 (2019) 108026

Contents lists available at ScienceDirect

Materials and Design

journal homepage: www.elsevier.com/locate/matdes

Influence of moisture and thermal cycling on delamination flaws in transparent armor materials: Thermoplastic polyurethane bonded glass-polycarbonate laminates

G. Rivers, D. Cronin *

Department of MME, University of Waterloo, 200 University Avenue West, Waterloo, Canada

HIGHLIGHTS

- A novel investigation identifying potential mechanisms of delamination failure in transparent armor laminates
- Proposed coupon-level specimens; manufactured from soda-lime-silica float glass, thermoplastic polyurethane, & polycarbonate
- Generated delamination from hygrothermal-aging and thermal cycling, attributed to changing polyurethane adhesion
- Failure mode transition, from bulk-cavitation to interfacial adhesion failure, with increasing moisture conditioning
- Results provide a treatment and methodology to assess potential for delamination in transparent armor laminates

GRAPHICAL ABSTRACT

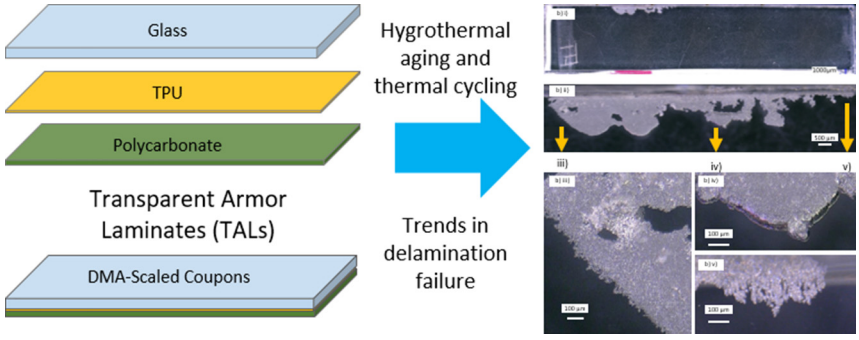

ARTICLE INFO

Article history:
Received 15 May 2019
Received in revised form 7 July 2019
Accepted 8 July 2019
Available online 09 July 2019

Keywords:
Delamination
Transparent armor
Laminates
In-situ
Polyurethane
Hygrothermal aging

ABSTRACT

Transparent armor laminates (TALs), manufactured from layers of soda-lime-silica float glass, thermoplastic polyurethane, and polycarbonate, are known to suffer unpredictable delamination in ambient-condition service, interfering with their transparency and reducing operational lifespan. The nature of the mechanisms leading to delamination are not well known, and believed to be driven by exposure to moisture, thermal cycling, and stresses induced by differing thermal expansion of the layers. Herein, small-scale coupons of TAL laminates were hygrothermally aged for a variety of durations and moisture exposure geometries, then thermally cycled to investigate the onset of delamination. As duration of aging was increased, the mode of failure changed from cohesive void formation at high temperature (85 °C), to interfacial crack during less-extreme thermal cycling (0 °C to 70 °C). The progression indicated that the barrier to nucleating delaminations reduced with progressing moisture exposure, leading to less-selective initiation and increasingly contiguous growth of the delaminations. In this study, for the first time, delaminations were successfully and consistently produced in glass-polycarbonate laminates, the delamination failure mode was correlated with the degree of moisture exposure, and both a theoretical basis to guide further studies and a methodology to assess the delamination resistance of current and future transparent armor designs are suggested.

* Corresponding author at: Department of Mechanical Engineering, University of Waterloo, 200 University Ave. West, Waterloo, Ontario N2L 3G1, Canada.
E-mail address: dscronin@mecheng1.uwaterloo.ca (D. Cronin).

https://doi.org/10.1016/j.matdes.2019.108026

1. Introduction and background

Durable and reliable transparent armors are necessary to defeat kinetic strikes on combat vehicle surfaces, and the vanguard option for this is multi-material laminated panels [1–4]. Transparent armor laminates (TALs) utilize a combination of materials to produce a structure that disrupts incoming impactors, then provides containment and energy dissipation for impact debris [1,3,4]. The hard disruption layers are often composed of borosilicate glass or soda-lime-silica float glass while the containment layers are often structural polymers such as polycarbonate [2]. Various polymers are used as interlayer adhesives such as are Polyvinyl butyral (or PVB), ethylene vinyl acetate, ionomers, and thermoplastic polyurethane (TPU), which adhere the various structural layers together during normal use [5–13]. To be useful, these laminates must be effective not only at defeating projectile impacts, but also for providing unimpeded view for drivers and field operators. Unfortunately, if the layers debond from one another during service the resulting voids will reduce visibility [2]. Failure by delamination has been widely reported by laminate armor manufacturers and end users, although the causes are not well understood nor are the conditions which produce or enlarge the delamination over time. Identifying root causes of delamination formation and growth could provide a means to prevent these failures, which would reduce maintenance costs and the risk to those whose lives are safeguarded by TALs.

Throughout the lifespan of a TAL, it has the potential to be exposed to a wide variety of environmental conditions, such as vibration, ultraviolet light exposure, temperature changes that may be rapid or repetitive, and moisture [7,8,14–23]. Each has the potential to alter the adhesive bonding layer such that a delamination has a higher probability of forming and enlarging. For example, moisture, UV light, and solvents can alter the chemical nature of polyurethane and thus its physical characteristics and adhesive capacity [7,8,16,17,21]. Relatedly, moisture absorption leading to hygrothermal aging and repeated temperature cycles can produce thermophysical aging, disruption of internal hydrogen bonding, and plasticization, especially when crossing the glass transition of the adhesive [14,15,18,21–23]. Further, changes in temperature may lead to debonding due to stresses imparted by mismatches in coefficients of thermal expansion between armor layers [19,20].

At present, there is a paucity of data regarding the conditions that may lead to delamination in a glass-polycarbonate laminate, and no test standard for this specific mode of failure. Previous research into the aging and failure of TALs is limited, with few studies focusing on delamination driven by hygrothermal aging and temperature fluctuations [19,20], and no recent peer-reviewed studies found in the open literature, with anecdotal reporting from investigations by end users and manufacturers indicating that moisture adsorption and temperature change are involved. Related laminate composites such as automotive safety glass or architectural glass laminates have been studied, although they often contain differing structures and chemistries; such research often reports the general effect of environmental factors on inter-layer adhesives commonly used in TALs [5–8,10,11,14–18,21,24]. In these studies, dynamic mechanical analysis to observe the influence of treatments on the mechanical nature of the materials has been occasionally employed [7,21].

In this study, temperature cycling and hygrothermal aging were performed as delamination-motivating antagonist conditions, using small-scale coupons of 3-layer TALs composed of soda-lime glass, thermoplastic polyurethane, and polycarbonate. The specimens were thermally cycled in a dynamic mechanical analyzer and evaluated for the initiation and propagation of delaminations, presenting a first demonstration of controlled and consistent delamination initiation in TALs.

2. Materials and methods

Small-scale 3-ply coupons of armor material test-laminates for this study (Fig. 1a) were manufactured using an autoclave process by Prelco Inc. according to methods and specifications used for full-scale transparent armor products. Specimens were composed of one layer each of soda-lime-silica float glass (2.7 mm thick Pilkington Optifloat Clear glass, Q3, Pilkington/Nippon Sheet Glass Co., Laurinburg, NC, USA), aliphatic thermoplastic polyurethane (Krystalflex 505, Huntsman, Mississauga, Canada), and polycarbonate (Makrolon, Bayer, Pittsburgh). The overall sample dimensions (length and width) were selected for compatibility with a Dynamic Mechanical Analyzer (TA-Instruments Q800) in three-point bending mode. Layer thicknesses were selected based on available source material, and with a goal to place the estimated location of the neutral bending axis of the laminated beam as close as possible to the same location, proportionally, as would be found in a three-ply full-scale armor panel, illustrated in Fig. 1b).

Specimens were separated into 9 groups subjected to differing hygrothermal aging ("HT-Aging", Table 1), and then exposed to different thermal treatments after aging (Table 2). Groups of specimens were HT-aged for one of four durations and one of three geometries of moisture ingress. Groups A and B were not aged, by isolating in a sealed bag and storing until testing. The remaining groups were aged in deionized water (DI-water, 15.5 to 17.2 Ω·cm resistivity) at 45 °C for 1008 h (42 days) (Groups C and D), 1200 h (50 days) (Groups E and F), or 1680 h (70 days) (Groups G, H and I). The durations used in this study were identified in an unpublished pilot study. Initial HT-aging for 50 days produced small delaminations. Reducing the aging time to 42 days, the smallest aging time reported in this study, ensured bracketing of the initiation of damage in the pilot study. The 1200 hour and 1680 hour HT-Aging groups were further subdivided based on moisture ingress geometry: one half were in contact with the water without restriction so that water could diffuse into the TPU along the entire specimen perimeter (Perimeter-Aging, Groups F and I), while the other half had a silicone putty seal applied around the perimeter of the sample prior to aging (Seal-Aging, Group G), and to restrict the entry of the water to an approximately 2 mm section of the TPU edge (Aperture-Aging, Groups E and H). A subset of specimens was further modified with a mechanical cut using a scalpel blade (Groups A, B, C), purposely introduced to the edge of the TPU layer, after lamination. This scenario introduced pre-damage to the adhesive layer and was intended to investigate whether existing localized damage would spread when thermally cycled.

After aging, specimens were exposed to thermal conditioning (Table 2). The first condition (1) thermally cycled at 20 °C per minute between 0 °C and 70 °C by DMA and monitored by cycling at 0.8% flexural strain at 1 Hz, with 15-min dwells at high and low temperature. This temperature range was identified from automotive literature for measured vehicle interior temperatures resulting from solar heating [25]. DMA cycling was performed 10 times per specimen and the specimens were sealed in plastic wrap prior to cycling, to prevent drying in the nitrogen purge atmosphere. In a second thermal treatment (2), the bath-cycled specimens were submerged in well-stirred baths, respectively maintained at 70 °C and 0 °C by a hot-plate and ice. Specimens were kept in the bath for 5 min per cycle and transferred between baths quickly to maximize thermal shock; specimens were bath-cycled 12 times each. In a third thermal treatment (3), specimens from Groups A, B, and C were placed in vacuum sealed bags and submerged in a stirred water bath at 85 °C for 3.5 h. Prior to and after thermal cycling, specimens were photographed with a scale bar for comparison, and measurements of the introduced cuts were made by image analysis (ImageJ). Select specimens were imaged in high resolution by an Opto-Digital Microscope ("ODM", Keyence VHX-5000, Keyence, Japan).

3. Results

3.1. High-temperature void formation in No HT-Aging and 1008 hr HT-Aging specimens

The No HT-Aging specimens were transparent prior to thermal conditioning, while the 1008 hr HT-Aging specimens displayed a gradient

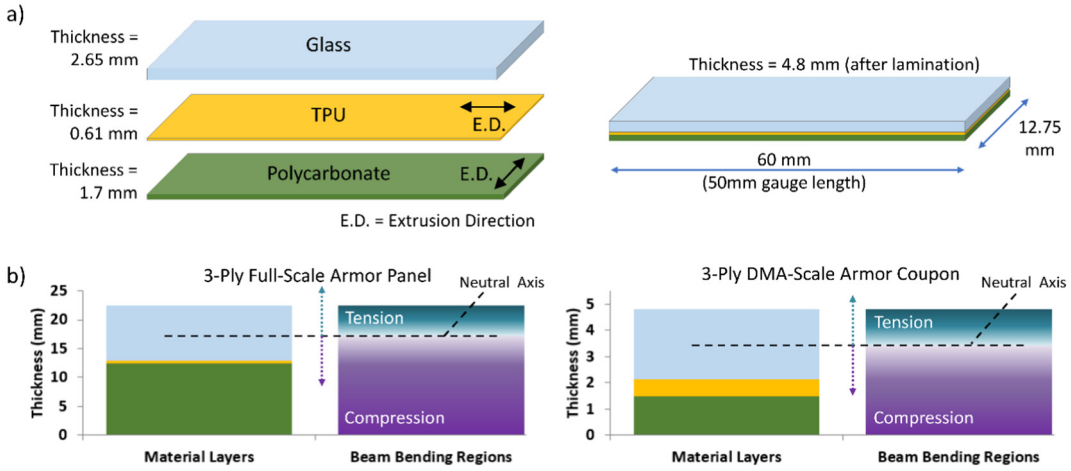

Fig. 1. a) Schematic of DMA-scale Transparent Armor Laminate coupons. b) Bending regions plotted next to material layers for full scale and coupon scale 3-ply armor laminates. "Tension" and "Compression" listed based on differential thermal expansion stresses in heated condition.

of haze inward from the edge of the specimen, in the TPU layer, indicating the intrusion of moisture. This haze was retained after thermal conditioning, and later faded as specimens were dried. After thermal conditioning by cycling between 0 °C and 70 °C, the No HT-Aging and 1008 hr HT-Aging specimens did not demonstrate the formation of voids or delaminations. Similarly, there was no growth of the mechanically-induced notches in this temperature range.

Higher temperature exposure without thermal cycling was then investigated. The No HT-aging and 1008 hr HT-Aging specimens were soaked in water for 3.5 h at 85 °C, and monitored for signs of failure. Both groups formed bubble-like smooth-surfaced voids (Fig. 2), though the number of voids per specimen varied, ranging from one to twenty.

Prior to exposure at 85 °C, it was observed that two of the No HT-Aging specimens (e.g. Fig. 3a and b) displayed small optical inhomogeneities in the bonding layer (Fig. 3a-ii and b-ii, schematic in a-iii and b-iii). Following exposure to 85 °C (Fig. 3a-iv, b-iv), a void formed at the location of the inhomogeneity, which was imaged by microscopy (Fig. 3a-v and b-v). Under ODM (Fig. 3b-v, b-vi), the structure that produced the inhomogeneity was still present, with minimal in-plane deformation, in the surface of the void. This indicated that the inhomogeneities were some physical structure that acted to nucleate the formation of a void under these conditions. Some suggested forms of these structures are: a thin layer of contamination at the PC-TPU interface, a zero-thickness (or "kissing contact") delamination at the PC-TPU interface, or a thin fracture in the TPU layer that leaves a thin film of TPU on the PC after delamination [26–28].

Voids also formed near the edge of the specimen, sometimes at locations correlated with small observed bonding flaws at the boundary of the specimen (blue arrows, Fig. 3a-i and a-iv). Similarly, under these conditions the purposely included mechanical damage to the TPU grew into similar voids (green arrow, Fig. 3a-i and a-iv). Thus, similar to the observed inhomogeneities, larger scale flaws acted as nucleation sites for void formation. However, voids formed in locations away from the edge of the specimen, and without recorded observation of an inhomogeneity. And so, although void formation appears to be influenced by the presence of localized inhomogeneities, void formation did not appear to be wholly dependent on those features. Thus, it is reasonable to state these voids represent a failure of the TPU itself, which can be locally influenced by boundaries and bonding flaws, which may contribute to the variability in number and position of the resulting voids.

Observation of the voids were also made via ODM, perpendicular to the other specimen orientations, through the edge of No HT-Aging specimens exposed to 85 °C (Fig. 4a and b). This view captured the as-manufactured edge of the specimens, which featured TPU "squeeze-out", machining marks on the PC edge, and small features on the glass-edge from the fracture-cutting. With the images taken such that the ODM focal plane was positioned at the voids, these other features appear out of focus, complicating the view. However, the observations indicate that the smooth bubble-like voids of interest could form at either the TPU-Glass interface, the TPU-PC interface, or in the bulk of the TPU layer.

Table 1
Specimen hygrothermal aging treatments. Each group contained 3 replicates.

Group	Test description	TPU mechanical damage	Thermal treatment (Table 2)	Located in results section:
A	No HT-Aging	Y	(1) 0–70 °C cycle, (3) 85 °C shock	3.1, 3.4
B	No HT-Aging	Y	(2) 0–70 °C shock, (3) 85 °C shock	3.1
C	1008 h HT-Aging[a] Full perimeter exposure	Y	(1) 0–70 °C cycle, (3) 85 °C shock	3.1, 3.4
D	1008 h HT-Aging[a] Full perimeter exposure	N	(2) 0–70 °C shock	3.1
E	1200 h HT-Aging[a] Aperture exposure	N	(1) 0–70 °C cycle	3.2
F	1200 h HT-Aging[a] Full perimeter exposure	N	(1) 0–70 °C cycle	3.2
G	1680 h HT-Aging[a] Sealed	N	(2) 0–70 °C shock	3.3
H	1680 h HT-Aging[a] Aperture exposure	N	(2) 0–70 °C shock	3.3
I	1680 h HT-Aging[a] Full perimeter exposure	N	(1) 0–70 °C cycle	3.3, 3.4

[a] HG Aging at 45 °C.

Table 2
Thermal treatments of specimens.

Treatment [#]	Description	Duration [#]	Heating rate [°C/min]	Temperature [°C]	
				Max	Min
1	DMA-cycled	10 cycles	20 (cycle)	70	0
2	Bath-cycled	12 cycles	Immersion (shock)	70	0
3	Bath 85 °C	3.5 h soak	Immersion (shock)	85 °C	N/A

3.2. Instances of delaminations from thermal cycling of 1200 hr HT-Aging specimens

Similar to the 1008 hr HT-Aging specimens, the 1200 hr HT-Aging specimens displayed gradient of haze in the TPU layer following aging. In the 1200 hr Aperture-Aging specimens there was a notable semi-circle of haze near the aperture. In the 1200 hr Perimeter-Aging specimens the gradient was around the full perimeter, and was more opaque and more extensive than in the 1008 hr HT-Aging specimens. After thermal conditioning by cycling between 0 °C and 70 °C, the 1200 hr Aperture-Aging specimens did not develop visible delaminations in any replicates. However, the 1200 hr Perimeter-Aging specimens developed a small number of delaminations at the edge of the specimens after thermal cycling, seen in Fig. 5a), and presented under magnification in Fig. 5b) and c).

Features of these delaminations included: 1) surfaces that were primarily large semi-transparent areas with a hazy texture; 2) surfaces that displayed sub-regions with differences in opacity; 3) small entrapped smooth-surfaced bubble-like voids; 4) linear striations observable as opacity differences in the delamination surfaces; and 5) the boundary of the delaminations were smooth with few interdigitations, and in one area featured a smooth-surfaced bubble-like perimeter (Fig. 5c). The differences in opacity and the associated striations in one section of the delamination have been annotated in an enlarged inset in Fig. 5c). Note that these opacity-striations were identified to be in the extrusion direction of the TPU adhesive layer.

3.3. Two types of delaminations from thermal cycling of 1680 hr HT-Aging specimens

All 1680 HT-Aging specimens displayed more-extensive hazing of the TPU than their 1200 hr counterparts, in the same patterns based on moisture ingress geometry; 1680 hr Perimeter-Aging specimens were nearly uniformly and intensely hazed throughout with only a slight gradient visible. In 1680 hr HT-Aging specimens, thermal cycling between 0 °C and 70 °C produced one of two types of delaminations based on the moisture-infiltration mode (Fig. 6a and b, respectively; Fig. 7a and b, respectively). Features shared by the delaminations in the 1680 hr HT-Aging groups, regardless of aging geometry, include: 1) surfaces that were primarily a "sugar-grain" texture with only minor variations across the surface; and 2) boundaries that had either a dendrite-like rough character, a bubble-like smoothness, or highly interdigitated "fingering" that is reminiscent of adhesive pull-off patterns [29]. The Aperture-Aging and Perimeter-Aging delaminations differed primarily in the distribution, continuity, and size of these delaminations. Aperture-Aging delaminations (Fig. 6a i-iii) displayed less continuity, less total area, and less localization than the Perimeter-Aging delaminations (Fig. 6b i-iii). This was consistent across replicates (Aperture-Aging in Fig. 7a-i to a-iii) and Perimeter-Aging in Fig. 7b-i) to b-v)). Interestingly, based on measurements made via the ODM based on focal length these highly-aged delaminations occurred at the Glass-TPU interface.

Additionally, the 1680 hr Aperture-Aging delaminations (Fig. 7a i-iii) displayed striations in the sugar-grain texture of the largest delamination cluster (annotated with red arrows). Linear clusters of small delaminations were arrayed alongside the large delamination, following the paths of the striations. It was noted that these striations were in the extrusion direction of the TPU adhesive layer. The 1680 hr Perimeter-Aging specimens (Figs. 6b i-iii, 7b i-iii) did not present these striations or linear clusters. Interestingly, whereas the 1680 hr Aperture-Aging delaminations were often not in contact with the edge of the specimens, the 1680 hr Perimeter-Aging delaminations typically presented a substantial contact with the specimen edge.

Fig. 8 presents the 1680 hr Perimeter-Aging specimen, imaged in two locations (the first in parts a) and the second in parts b)) by ODM under two imaging settings ("full-ring polarized light" in part i) of each, and "coaxial polarized light with High Dynamic Range Enhancement" (HDR) in part ii) of each). In Fig. 8a-i) and b-i) under full-ring polarized light there were small delaminations identified, surrounded by faint distortions. These distortions became more apparent in part ii) of each, under HDR enhancement, with similar features revealed in other locations nearby.

To test the effectiveness of the seal used in aperture testing, three specimens were fully-sealed without an aperture, and hygrothermally aged in 45 °C water for 1680 h ("1680 hr Seal-Aging" specimens). After aging the specimens were slightly hazy, uniformly across the specimen, and far less substantially than the Aperture-Aging and Perimeter-Aging specimens. This indicates that the seals were effective and that the polymer morphology of the TPU interlayer was affected by the long-term storage at 45 °C without moisture infiltration. In either case, thermal cycling of these specimens between 0 °C and 70 °C by bath immersion did not produce any voids or delaminations.

3.4. Influence of HT-aging duration on mechanical properties during thermal cycling

Three types of specimens (No HT-Aging, 1008 hr H-T Aging, and 1680 hr H-T Perimeter-Aging specimens) were thermally cycled from 0 °C to 70 °C during dynamic mechanical analysis. For ease of comparison, the second thermal cycle of each scan has been displayed (storage modulus in Fig. 9a-i) and loss modulus in Fig. 9a-ii)). The full trend over ten applied thermal cycles is plotted in Fig. 9b), with storage and loss moduli shown in parts i) and ii), respectively.

As the specimens were aged for longer periods, the sensitivity of the storage modulus to temperature change increased, indicating increased

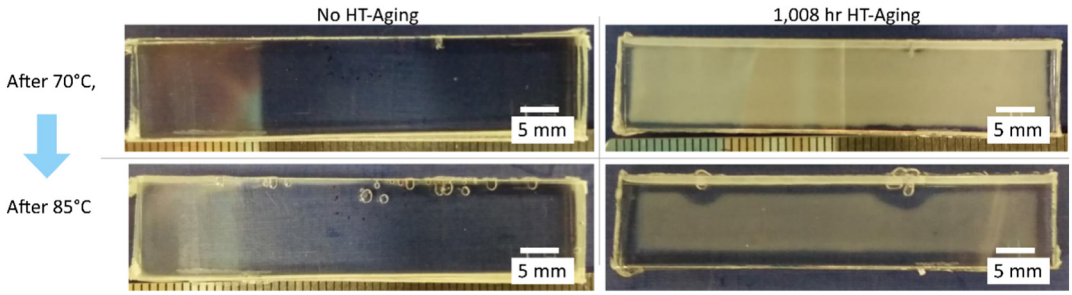

Fig. 2. No HT-Aging and 1008 hr HT-Aging specimens before and after 85 °C exposure, (scale in mm).

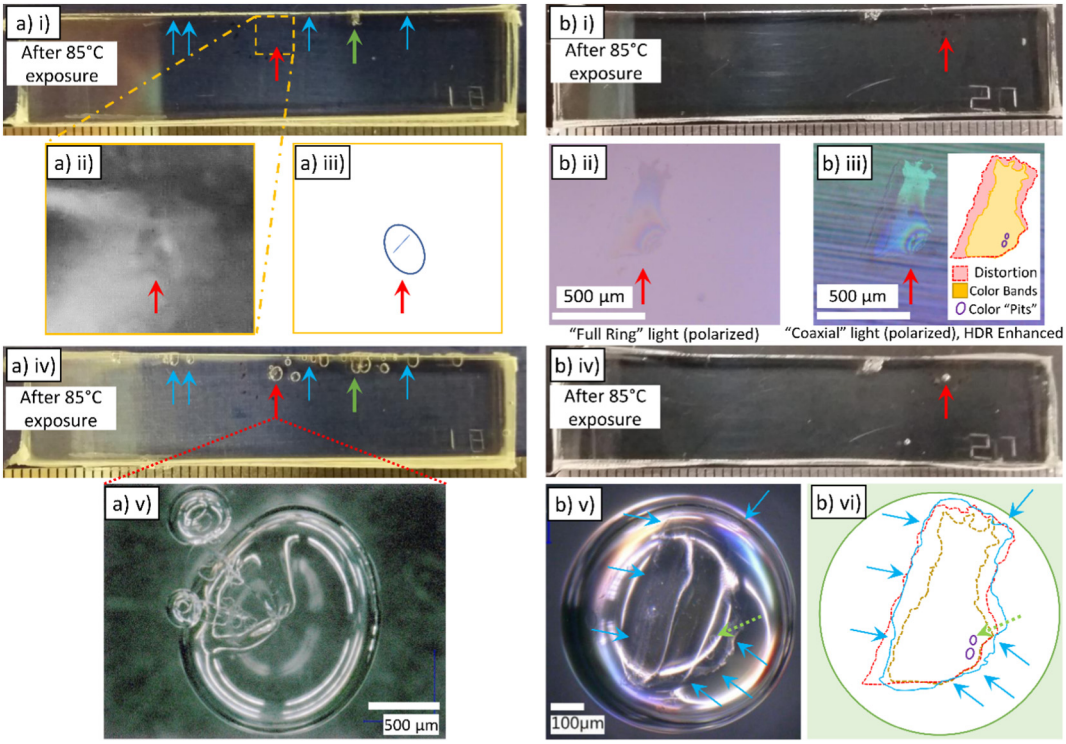

Fig. 3. Two specimens imaged by photography and ODM, before and after exposure to 85 °C. Annotations track locations within each: a-i) specimen before thermal conditioning, and at higher magnification; a-ii), presenting a small optical inhomogeneity; a-iii) schematic; a-iv) specimen after 85 °C treatment, a bubble-like void (magnified in a-v) nucleated at the observed inhomogeneity. Parts b-i) through -vi): similar presentations of another specimen, with initial inhomogeneity feature observed and imaged by ODM, and tracings comparing the inhomogeneity to markings on the resulting void.

plasticity of the composite, believed to be a result of increased plasticity of the TPU interlayer. The shape of the loss modulus curve, in terms of peaks within the curve and the area of the hysteresis curve, was also highly influenced by the aging. Over thermal cycling, in Fig. 9b i) and b ii), the observed shifts in both moduli clearly show that the No HT-Aging specimen displays only minor changes, while the others display cycle-to-cycle shifts that increase with HT-aging duration. Specimens were wrapped in thin plastic barrier material prior to DMA thermal cycling, and displayed no visible signs of drying during thermal cycling.

4. Discussion

The experimental results confirm literature expectations that delamination in aged TAL materials is a function of both the temperature exposure and the moisture exposure of the polymer [19,20]. The results primarily indicate that as moisture exposure increases from minimum to maximum studied exposures, the void and delamination behavior transitions from: 1) smooth-sided voids at low moisture content, which do not form during 0 °C to 70 °C cycling, requiring high temperatures of 85 °C to initiate from a small number of locations; to 2) rough-textured continuous interfacial delaminations that originate during cycling between 0 °C and 70 °C, presenting an apparent mixture of crack-tip advancement and widespread nucleation. This progression can be seen in a collection of specimen images arranged by HT-aging group and thermal conditioning (Fig. 10).

Our experimental findings allowed us to draw a connection to the theoretical framework of cohesion and adhesion failure discussed by Creton et al., which provided the basis to reframe delamination from a problem of stresses and polymer degradation to a problem of stresses and changing adhesion parameters from microstructural evolution [30]. The two primary observed modes of failure, bubble-like voids and rough-textured continuous interfacial delaminations, appear to be geometrically analogous, respectively, to "Sequence C" and "Sequence A" failures, as described by Creton et al. Sequence C is characterized by bulk cavities formed when hydrostatic tension exceeds the interlayer's elastic modulus, "E", causing local yielding. Sequence A is characterized by nucleation, growth, and consolidation of a population of crack-like interfacial cavities, when the local driving force of the stress field exceeds the critical energy release rate that characterizes interfacial adhesion, "G_0" [30]. That study reported on debonding of an axially loaded

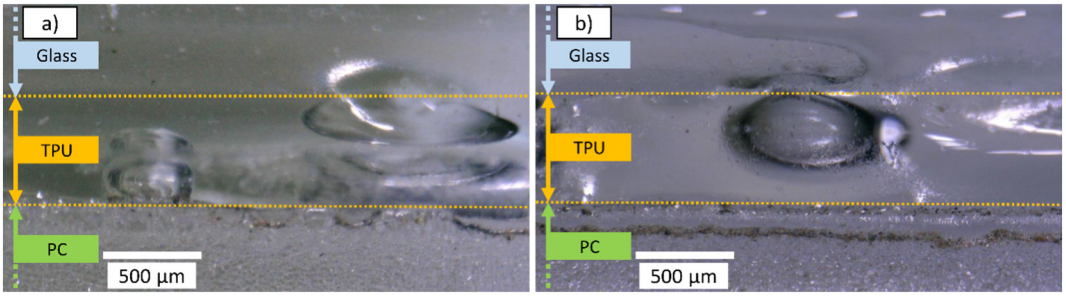

Fig. 4. ODM of No HT-Aging specimens after 85 °C heat treatment, viewed from the edge looking down at the three layers. Edges have been annotated, and bubble-like voids can be seen.

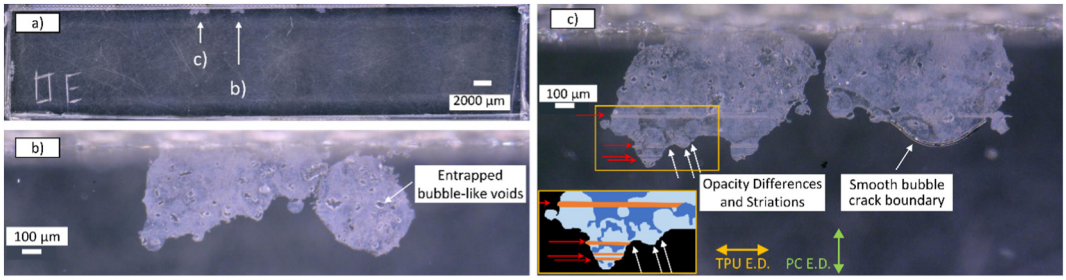

Fig. 5. ODM of a 1200 hr Perimeter-Aging specimen after 0 °C to 70 °C thermal cycling. a) Full-specimen, with annotations of the higher magnifications in parts b) and c). An inset tracing of one section is included to highlight the regions discussed.

adhered layer with varying adhesion due to surface treatments. If we consider that differential thermal expansion of the glass and polycarbonate layers would apply the stress field to the adhesive interlayer of TALs, and thus provide a driving force in the same manner as the uniaxial loading of Creton et al., this implies that the localized interfacial debonding observed as inhomogeneities may be acting as local stress concentrators, resulting in void formation at their locations under high thermal stress loading in specimens with minimal HT-Aging. Additionally, it implies that exposure to moisture during long-duration hygrothermal aging is lowering the critical failure mode ratio (G_0/E) for the TPU interlayer, in the same manner as the surface treatments applied by Creton et al. [30].

Intermediate (1200 h HT-Aging) exposure to moisture, followed by thermal cycling between 0 °C and 70 °C, resulted in small delaminations that presented intermediate forms between the two above conditions. A moderate duration of exposure to moisture resulted in small delaminations with translucent surfaces. These small delaminations presented striations that influenced the delamination perimeter and appeared with lightly textured translucent surfaces containing small smooth and transparent regions. As such, they appear to have an intermediate surface quality between the "sugar grain" texture of the highly aged specimens and the smooth voids of the specimens without water exposure. When water influx was restrained by a seal and aperture in the intermediate (1200 h HT-Aging) specimens, no delaminations were seen. This indicates that the moisture exposure of the 1200 hr Aperture-Aging specimens was below some critical amount to produce the onset of delamination under the 0 °C to 70 °C thermal cycling condition, met by the 1200 hr Perimeter-Aging specimens.

Similarly, when the moisture ingress of the long-term (1680 h HT-Aging) specimens was restricted via a seal and aperture, the delaminations were reduced in their size, and connectivity, indicating that increased moisture content is also correlated with the severity of a delamination under the same temperature conditions. These delaminations appeared to prefer nucleating at striations following the TPU extrusion direction, indicating again the presence of nucleation sources, such as surface or bulk microstructures or contaminates in the TPU interlayer, imparted by the film manufacture.

The optical distortions found in the 1680 hr Perimeter-Aged specimens (Fig. 8) were found near the main delamination, and correlated with the small delaminations that nucleated near the "leading edge" of the delaminations. This may be a stress concentration effect, resulting in new delaminations being subsumed by the growing main delamination; a likely source of the "sugar grain" texture. It is hypothesized that these small distortions may be localized microstructure changes to the TPU, possibly produced in part by the moisture infiltration and the resulting plasticization [14], or by cyclic strain from the thermal cycling, or from various diffusion and crystallization processes within the plasticized TPU during thermal cycling [31]. These changes were not seen in less-aged specimens, indicating that the formation of the microstructures producing the optical distortions, and the resulting delaminations, are moisture-dependent.

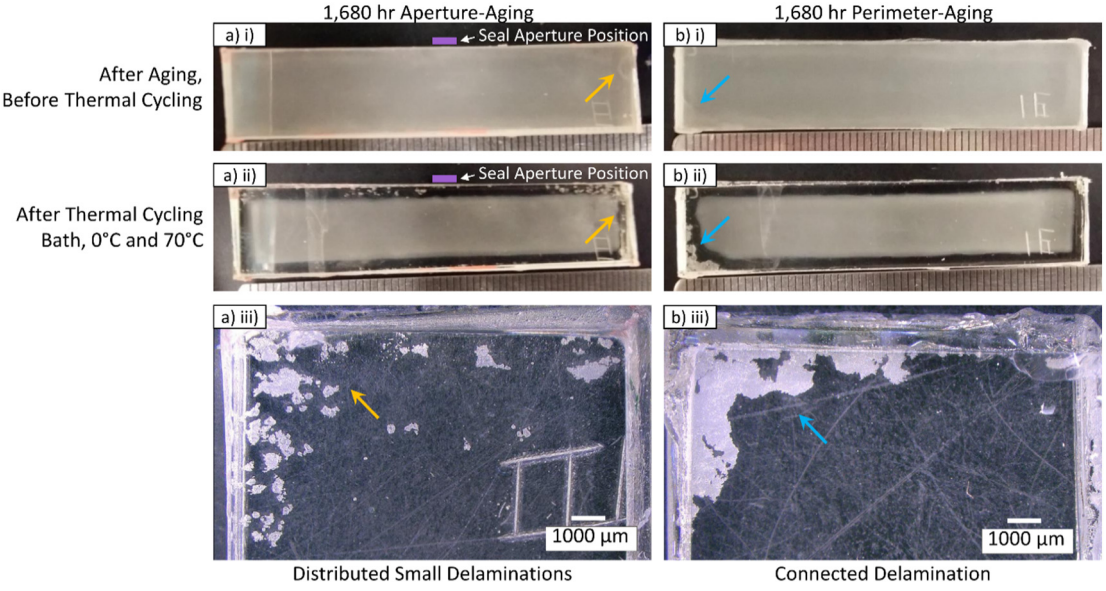

Fig. 6. Examples of specimens HT-aged for 1680 h with two geometries of moisture exposure, before and after thermal cycling (0 °C to 70 °C by repeated bath immersion). a) 1680 h Aperture-Aged i) before thermal cycling, with a faint radial gradient originating from the seal aperture position (purple annotation), and a small semi-circle inhomogeneity tracked by yellow annotated arrow (dimensions in mm); ii) after thermal cycling; and iii) in close-up after thermal cycling. b) 1680 h Perimeter-Aging i) through iii): similar presentation, with a small inhomogeneity tracked by blue annotated arrow.

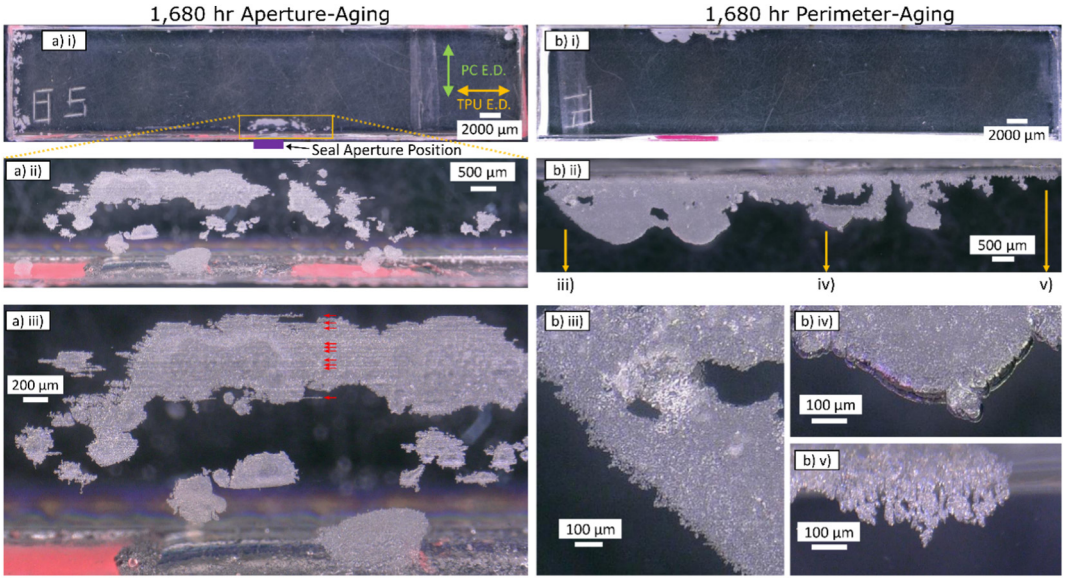

Fig. 7. 1680 hr HT-Aging specimens after thermal cycling. a-i) Aperture-Aging specimen with the extrusion direction of the polymer layers annotated, and an annotation showing the position of magnification; a-ii) presenting a delamination cluster; a-iii) presents further magnification, with a "sugar-grain" delamination surface texture, and striations in TPU extrusion direction (annotated by red arrows). b-i) through -v) similar presentation of Perimeter-Aging specimen, with: iii) "snowflake" dendritic patterns with no directional bias; iv) "sugar-grain" texture ending at a bubble-like crack tip perimeter; and v) highly interdigitated pull-off patterns.

The processes of annealing and crystallinity refinement in TPUs are both correlated with the mechanical properties of the TPU and adhesion on glass, which correlate with the bonded TPU properties of E and G_0 [32,33]. TPU hard-segment (HS) crystals do not bond to glass as well as TPU soft-segments (SS) [32,33]. Moisture adsorption reduces HS crystal stability, allowing the HS components to diffuse out of small as-annealed crystals and undergo cold-crystallization during exposure to elevated temperatures [14,31]. If HS segments were free to diffuse and recrystallize at laminate interfaces, this would reduce the adhesion strength of the TPU (reducing G_0, and G_0/E in turn), resulting in a change in failure form, and the reduced temperatures necessary to produce delaminations.

Thus, we hypothesize that TPU microstructure phase development may be one of the fundamental mechanisms of delamination in TPU-assembled TALs. Increases in temperature and differing coefficients of thermal expansion of the TAL layers produce thermally-induced shear stresses in all three layers, as expected. This effect is then coupled with changing adhesion properties from a non-chemical moisture-assisted material evolution of the TPU, as the TAL is exposed to moisture and to thermal conditioning. It is likely that this coupled effect of both

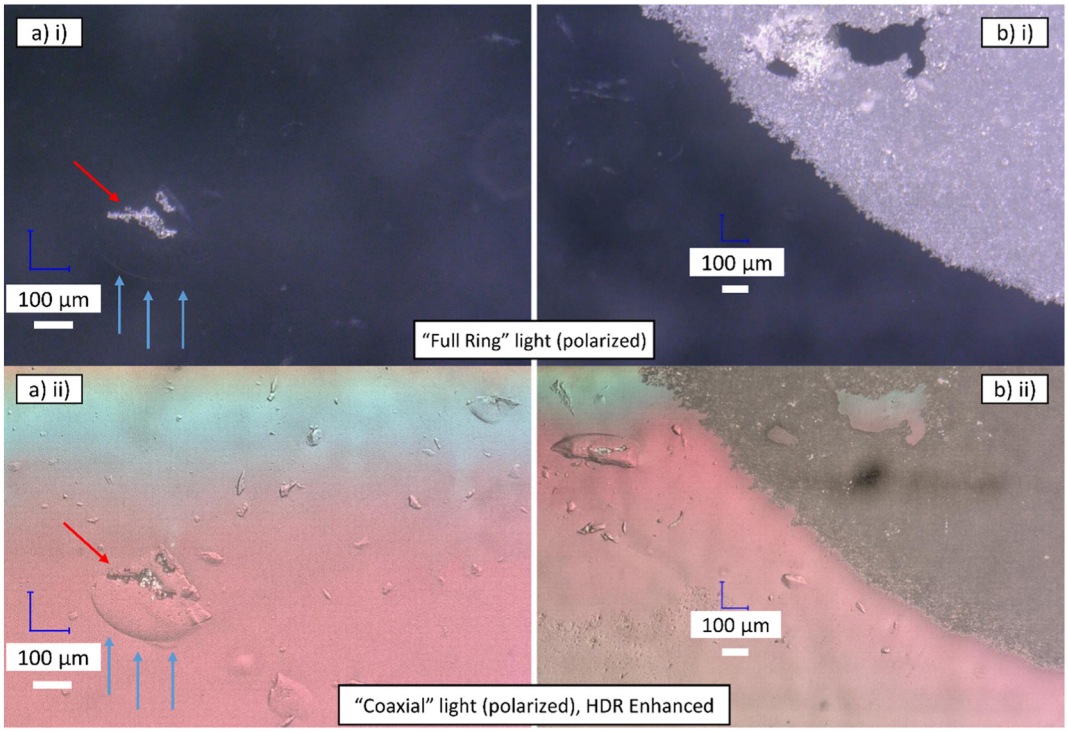

Fig. 8. 1680 hr Perimeter-Aging specimen, imaged by ODM under two imaging settings, in two locations. Optical inhomogeneities correlate with the formation of small delaminations.

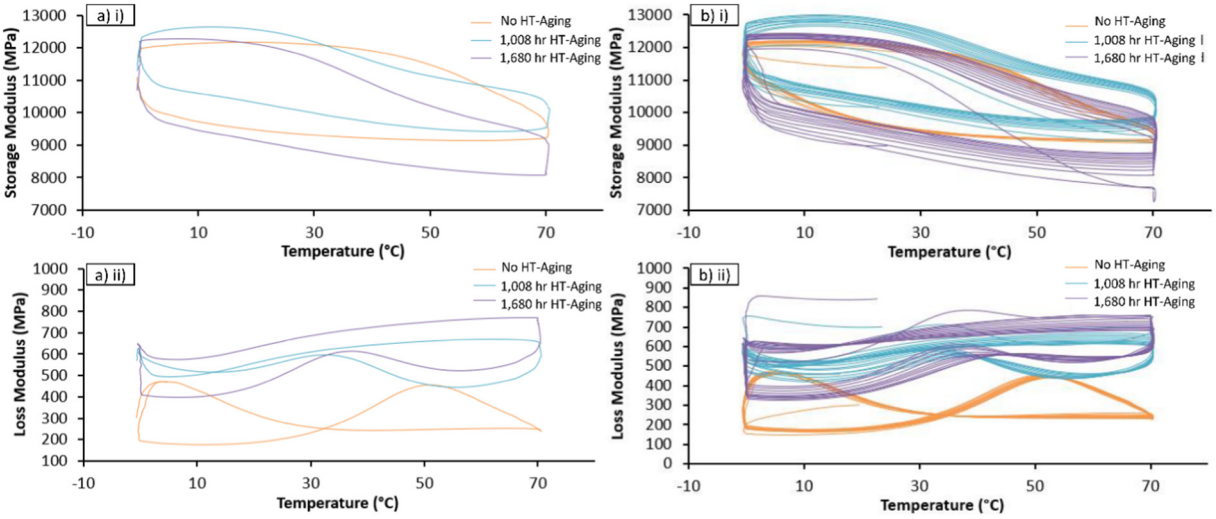

Fig. 9. Dynamic Mechanical Analysis (DMA) of No HT-Aging, 1.008 h HT-Aging, and 1680 hr Perimeter-Aging specimens. For clarity of comparison, the second cycle of each is presented in a-i) storage modulus and a-ii) loss modulus. To observe the trends as thermally cycled, all cycles are presented in b-i) storage modulus and b-ii) loss modulus.

thermal stresses and adhesion loss, interacting to produce a progression of failures under differing conditions, explains why previous studies have not resolved the underlying nature of delaminations in TALs. This may also explain why delaminations can occur at lower temperatures than those utilized in this study, given sufficient exposure time.

In future studies, the inclusion of lower temperature conditions is recommended for the minimum temperature condition, including as low as −40 °C, to be combined with a variety of maximum temperatures. Finite element analysis to investigate stress distributions in the part are recommended, which may help further explain the nature and extent of the delamination initiation. Image analysis should be employed, to quantify the geometry of the interfacial delaminations. Direct observation of the TPU microstructure at the delamination sites should be considered in future studies, for example though tapping mode atomic force microscopy. This is to be combined with longer-term hygrothermal and thermal-conditioning studies, to determine the necessary conditions and mechanisms of delamination onset at lower temperatures.

5. Conclusion

Progression of delamination in DMA-scaled laminate coupons of transparent ballistic armor materials is presented, demonstrating a shift in thermally-induced failure modes as moisture exposure increases. Initially, with no moisture exposure or minimal exposure (1008 h), laminate failure did not occur during thermal cycling from 0 °C to 70 °C, instead requiring multiple hours at 85 °C to initiate failure. These were small, smooth-walled, and transparent cohesive failure voids, which were observed to sometimes nucleate from pre-existing inhomogeneities in the layer interfaces. As moisture exposure was increased it became possible to induce delaminations with thermal cycling from 0 °C to 70 °C. In the intermediate moisture content (1200 h Perimeter-Aging), the surfaces of the induced failures were smooth and translucently hazy, presenting differences in opacity, as well as presenting apparent striations that followed the as-manufactured rolling-direction of the TPU film. Further exposure to moisture (1680 h Aperture-Aging) resulted in delaminations with a crack-like adhesive-

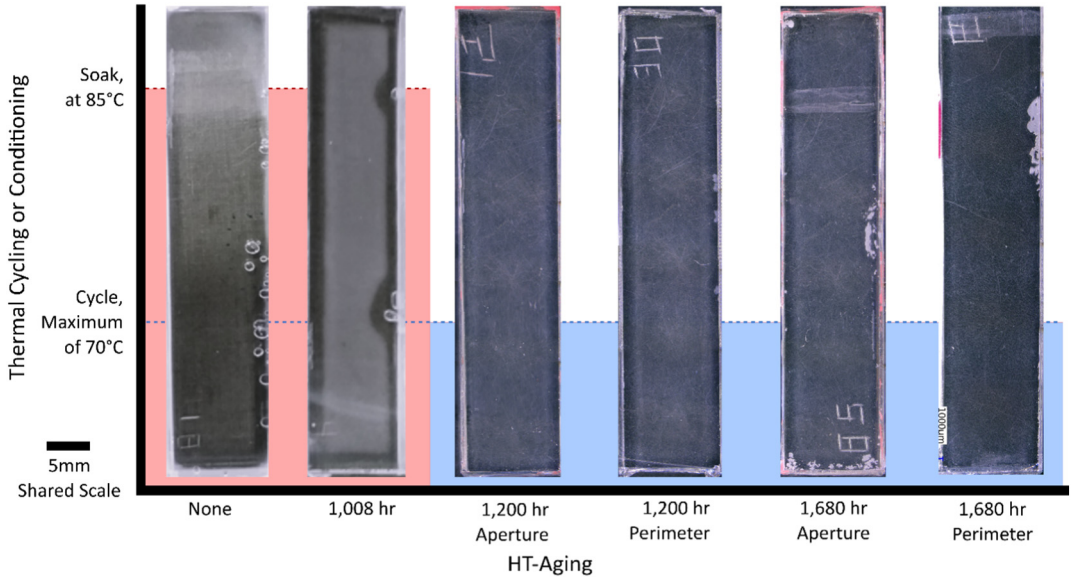

Fig. 10. Exemplar test specimens at a common scale, arranged left-to-right according to increasing moisture exposure during HT-Aging. No HT-Aging and 1008 h HT-Aging formed bubble-like voids only after exposure to 85 °C. 1200 hr Aperture-Aging specimens displayed no delaminations, while 1200 hr Perimeter-Aging specimens display small delaminations with intermediate form. 1680 hr HT-Aging specimens display interfacial delaminations, with Aperture-Aging resulting in disconnected "archipelagos", and Perimeter-Aging resulting in contiguous delaminations. In these last four groups, the total delaminated area visibly increased with increasing moisture exposure.

failure quality. These were arranged as an 'archipelago' of non-contacting but closely situated failures, scattered around the perimeters of specimens. These delamination fracture texture and clusters featured linear chains of striations, which followed the TPU rolling direction. In the highest studied moisture exposure (1680 h Perimeter-Aging), the delaminations were localized to large and highly connected delaminations, and did not display the striations seen in the other aging states. Combined, this indicates that long term exposure to moisture followed by exposure to thermal cycling is a progressing process, in which the barrier to nucleate and propagate delaminations is progressively reduced. A suggested mechanism for this is moisture-facilitated microstructure diffusion of the TPU, resulting in a moisture exposure dependent loss of adhesion under cold-crystallization conditions. This transition shifts the failure from bulk cavitation of the TPU under high thermal stress loading, to crack-like interfacial debonding at lower thermal stresses. Thus, this work presents insights into the progression of moisture-enabled delaminations of transparent armor panels, and new observations of the underlying processes that drive these failures, with a first demonstration of controlled and consistent delamination initiation in TALs.

CRediT authorship contribution statement

G. Rivers: Conceptualization, Methodology, Investigation, Formal analysis, Writing - original draft, Writing - review & editing. **D. Cronin:** Supervision, Methodology, Formal analysis, Data curation, Funding acquisition, Writing - original draft, Writing - review & editing.

Acknowledgments

The authors would like to thank the Natural Sciences and Engineering Research Council of Canada, Defence Research and Development Canada - Valcartier Research Centre, Prelco Inc., General Dynamics Land Systems-Canada and the National Research Council Canada for financial and technical support.

Data availability statement

The raw/processed data required to reproduce these findings cannot be shared at this time as the data also forms part of an ongoing study.

References

[1] S. Böhmer, Ageing of transparent armour – numerical simulations of FSP 20 mm on laminated glass, 2nd Workshop on Ageing Effects in Protective Systems, Components and Materials, May 15–17, 2018.
[2] M. Grujicic, W.C. Bell, B. Pandurangan, Design and material selection guidelines and strategies for transparent armor systems, Mater. Des. 34 (2012) 808–819.
[3] J. Parienté, Accelerated Aged Transparent Armor under Ballistic Impact, Renault Trucks Defense, 2018.
[4] Welker R., Forster S., and Hofmann T., "Aging of laminated glass - testing and analysis of polymeric components and interfaces", Workshop on Aging Effects in Protective Materials, May 16, 2018.
[5] Andreozzi L., Bati S. B., Fagone M., Ranocchiai G. and, Zulli F., "Weathering action on thermo-viscoelastic properties of polymer interlayers for laminated glass", Construction and Building Materials, 2015, 98, 15, p. 757–766.
[6] P. Del Linz, P.A. Hooper, H. Arora, Y. Wang, D. Smith, B.R.K. Blackman, J.P. Dear, Delamination properties of laminated glass windows subject to blast loading, Int. J. Impact Eng. 105 (2017) 39–53, https://doi.org/10.1016/j.ijimpeng.2016.05.015.
[7] M. Kothe, B. Weller, "Influence of Environmental Stresses to the Ageing Behaviour of Interlayer", Challenging Glass 4 and COST Action TU0905 Final Conference, 2014.
[8] J. Nicholas, M. Mohamed, G.S. Dhaliwal, S. Anandan, K. Chandrashekhara, Effects of accelerated environmental aging on glass fiber reinforced thermoset polyurethane composites, Compos. Part B 94 (2016) 370–378, https://doi.org/10.1016/j.compositesb.2016.03.059.
[9] Ranocchiai G., Andreozzi L., Zulli F., and Fagone M., "Effects of interlayer weathering on the structural behaviour of laminated glass structures", Challenging Glass Conference Proceedings, [S.l.], 5, p. 385–390, June 2016. ISSN 2589-8019, doi:https://doi.org/10.7480/cgc.5.2264.
[10] T. Serafinavičius, J.-P. Lebet, C. Louter, T. Lenkimas, A. Kuranovas, Long-term laminated glass four point bending test with PVB, EVA and SG interlayers at different temperatures, Procedia Eng. 57 (2013) 996–1004, https://doi.org/10.1016/j.proeng.2013.04.126.
[11] Vedrtnam A., "Experimental and simulation studies on delamination strength of laminated glass composites having polyvinyl butyral and ethyl vinyl acetate interlayers of different critical thicknesses", Defence Technology, 2018, 14, 4, p. 313–317, DOI: doi:https://doi.org/10.1016/j.dt.2018.02.002.
[12] B. Weller, M. Kothe, Ageing Behaviour of Polymeric Interlayer Materials and Laminates, Glass Performance Days, 2011.
[13] L.H. Zhang, X.H. Yao, S. Zang, Q. Han, Temperature and strain rate dependent tensile behavior of a transparent polyurethane interlayer, Mater. Des. 65 (2015) 1181–1188.
[14] Boubakri A., Elleuch K., Guermazi N., and Ayedi H. F., "Investigations on hygrothermal aging of thermoplastic polyurethane material", Materials and Design, 2009, 30, 10, p. 3958–3965, DOI: doi:https://doi.org/10.1016/j.matdes.2009.05.038.
[15] Boubakri A., Haddar N., Elleuch K., and Bienvenu Y., "Impact of aging conditions on mechanical properties of thermoplastic polyurethane" Materials and Design, 2010a, 31, 9, p. 4194–4201, DOI: doi:https://doi.org/10.1016/j.matdes.2010.04.023.
[16] Boubakri A., Guermazi N., Elleuch K., and Ayedi H. F., "Study of UV-aging of thermoplastic polyurethane material", Mater. Sci. Eng. A, 2010b, 527, 7, p. 1649-1654, DOI: doi:https://doi.org/10.1016/j.msea.2010.01.014.
[17] Boubakri A., Haddar N., Elleuch K., and Bienvenu Y., "Influence of thermal aging on tensile and creep behavior of thermoplastic polyurethane", Comptes Rendus Mécanique, 2011, 339, 10, p. 666–673, doi:https://doi.org/10.1016/j.crme.2011.07.003.
[18] R.N. Jana, H. Bhunia, Accelerated hygrothermal and UV aging of thermoplastic polyurethanes, High Perform. Polym. 22 (2010) 3–15, https://doi.org/10.1177/0954008308097460.
[19] Leighton K., Carberry J., Serafin W., Avery T., and Templeton D., "Transparent Armor for the New Standard in Transparent Battle Performance", U.S. Army's Tank and Automotive Command (TACOM), 2011, Technical Document # 21439.
[20] Pint E. M., Fleming J., Germanovich G., and Muggy L., "Addressing Ballistic Glass Delamination in the Marine Corps Tactical Vehicle Fleet", RAND Corporation, 2018, DOI:https://doi.org/10.7249/RR2285.
[21] Sakai K., and Nassar S.A., "Polycarbonate-to-polycarbonate single lap joints with polyurethane film adhesive", Automotive Composites Conference and Exhibition, 2017, pp. 19.
[22] C.S. Schollenberger, F.D. Stewart, Thermoplastic polyurethane hydrolysis stability, J. Elastomers Plast. 3 (1971) 28–56, https://doi.org/10.1177/009524437100300103.
[23] Yang B., Huang W. M., Li C., and Li L., "Effects of moisture on the thermomechanical properties of a polyurethane shape memory polymer", Polymer, 2006, 47, 4, p. 1348–1356, DOI:https://doi.org/10.1016/j.polymer.2005.12.051.
[24] Li X., Lu J., Luo J., Zheng H., and Shao G.Q., "Effects of cold plasma treatment on the performance of polyurethane laminated glass", Plasma Chemistry and Plasma Processing, 2014, 34, 1, p. 207–215, DOI:https://doi.org/10.1007/s11090-013-9494-0.
[25] W. Atkinson, W. Hill, The Heat Is On: Don't Leave your Chocolate Candy, Kids or Pets in a Parked Car, SAE, May, 2015http://www.sae.org/standardsdev/tsb/cooperative/int_temp.pdf.
[26] R.D. Adams, Nondestructive testing, in: L.F.M. da Silva, A. Öchsner, R.D. Adams (Eds.), Handbook of Adhesion Technology, Springer International Publishing, 2018https://doi.org/10.1007/978-3-319-55411-2_42.
[27] Jeenjitkaew C., Luklinska Z., and Guild F., "Morphology and surface chemistry of kissing bonds in adhesive joints produced by surface contamination", International Journal of Adhesion and Adhesives, 2010, 30, 7, p. 643–653, DOI: doi:https://doi.org/10.1016/j.ijadhadh.2010.06.005.
[28] P.N. Marty, N. Desaï, J. Andersson, "NDT of Kissing Bond in Aeronautical Structures", 16th World Conference on Nondestructive Testing, 2004.
[29] Fields R. J., and Ashby M. F., "Finger-like crack growth in solids and liquids", The Philosophical Magazine: A Journal of Theoretical Experimental and Applied Physics, 1976, 33, 1, p. 33–48, doi:https://doi.org/10.1080/14786437608221089.
[30] C. Creton, J. Hooker, K.R. Shull, Bulk and interfacial contributions to the debonding mechanisms of soft adhesives: extension to large strains, Langmuir 17 (2001) 4948–4954.
[31] Y. Yanagiharaa, N. Osaka, S. Iimori, S. Murayama, H. Saito, Relationship between modulus and structure of annealed thermoplastic polyurethane, Mater. Today Commun. 2 (2015) e9–e15, https://doi.org/10.1016/j.mtcomm.2014.10.001.
[32] Agrawal R. K., and Drzal L. T., "Adhesion mechanisms of polyurethanes to glass surfaces. Part II. Phase separation in polyurethanes and its effects on adhesion to glass", Journal of Adhesion Science and Technology, 1995, 9, 10, p. 1381–1400.
[33] Sánchez-Adsuar M. S., "Influence of the composition on the crystallinity and adhesion properties of thermoplastic polyurethane elastomers", International Journal of Adhesion and Adhesives, 2000, 20, 4, p. 291–298.